Structural Interactions Dictate the Kinetics of Macrophage Migration Inhibitory Factor Inhibition by Different Cancer-Preventive Isothiocyanates

ARTICLE *in* BIOCHEMISTRY · AUGUST 2012

Impact Factor: 3.02 · DOI: 10.1021/bi3005494 · Source: PubMed

BIOCHEMISTRY
including biophysical chemistry & molecular biology

Article

pubs.acs.org/biochemistry

Structural Interactions Dictate the Kinetics of Macrophage Migration Inhibitory Factor Inhibition by Different Cancer-Preventive Isothiocyanates

Gregg V. Crichlow,[†,⊥] Chengpeng Fan,[†] Camille Keeler,[‡] Michael Hodsdon,[‡] and Elias J. Lolis*[,†,§]

[†]Department of Pharmacology, [‡]Department of Laboratory Medicine, and [§]Yale Comprehensive Cancer Center, Yale University School of Medicine, New Haven, Connecticut 06510, United States

Supporting Information

ABSTRACT: Regulation of cellular processes by dietary nutrients is known to affect the likelihood of cancer development. One class of cancer-preventive nutrients, isothiocyanates (ITCs), derived from the consumption of cruciferous vegetables, is known to have various effects on cellular biochemistry. One target of ITCs is macrophage migration inhibitory factor (MIF), a widely expressed protein with known inflammatory, pro-tumorigenic, pro-angiogenic, and anti-apoptotic properties. MIF is covalently inhibited by a variety of ITCs, which in part may explain how they exert their cancer-preventive effects. We report the crystallographic structures of human MIF bound to phenethylisothiocyanate and to L-sulforaphane (dietary isothiocyanates derived from watercress and broccoli, respectively) and correlate structural features of these two isothiocyanates with their second-order rate constants for MIF inactivation. We also characterize changes in the MIF structure using nuclear magnetic resonance heteronuclear single-quantum coherence spectra of these complexes and observe many changes at the subunit interface. While a number of chemical shifts do not change, many of those that change do not have features similar in magnitude or direction for the two isothiocyanates. The difference in the binding modes of these two ITCs provides a means of using structure−activity relationships to reveal insights into MIF biological interactions. The results of this study provide a framework for the development of therapeutics that target MIF.

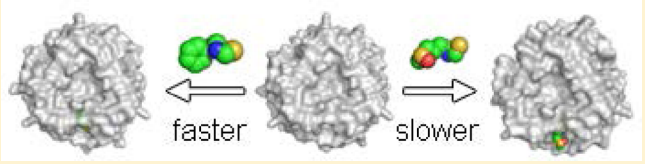

Macrophage migration inhibitory factor (MIF) is a widely expressed pro-inflammatory protein that is under investigation as a potential target for interventions against sepsis, autoimmune diseases, and cancer.[1−3] The tautomerase activity of MIF (EC 5.3.2.1) has been used for drug screening and inhibitor design. Compounds that inhibit MIF tautomerase activity have been found also to inhibit MIF biological functions in cell-based and in vivo experiments.[4,5]

However, there is a continuing debate about whether inhibition of enzymatic activity or antagonism of MIF−receptor interactions is the mechanism that results in decreased biological activity.[6,7]

Recently, proteomic studies that aimed to identify cellular proteins modified by isothiocyanates (ITCs) revealed MIF was specifically targeted.[8−10] Isothiocyanates make up a class of nutrients obtained through consumption of cruciferous vegetables, having well-known cancer-preventive properties.[11,12] The inhibition of MIF by these compounds provides an explanation of some salubrious effects of ITCs that are not explained by its other known cellular targets and activities.[10] Furthermore, oil containing phenylethylisothiocyanate [also known as phenethylisothiocyanate (PEITC)] has been found to be active against ulcerative colitis.[13] Although the target is not known in this study, it is interesting that MIF is implicated in colitis[1] as well as other pro-inflammatory diseases, and on the basis of the proteomics experiments, the target is likely to be MIF.

It has been found that consumption of isothiocyanate nutrients derived from cruciferous vegetables may reduce the risk of having cancer.[14−16] In particular, the isothiocyanates L-sulforaphane, abundant in broccoli, and PEITC, abundant in watercress, have anti-myeloma properties.[17] The mechanism of this protection has been found to be manifold, including genotoxic effects on tumor cells,[18] induction of redox-protective "phase 2" enzymes,[19,20] and inhibition of cytochrome P450-mediated production of toxic carcinogenic metabolites.[20] ITCs also target tumor cells directly via glutathione depletion and increased oxidative stress.[21] Although isothiocyanates have been found to be very beneficial nutritionally, not enough is known about proper dosage and timing of administration for them to be useful therapeutically. One group reported induction of bladder tumors in rats upon treatment with an isothiocyanate after induction of tumorigenesis via administration of a carcinogen,[22] although isothiocyanate intake prior to, or along with, carcinogen administration reduced the cancer risk in the same strain of rat.[23] Another group reported low concen-

Received: April 29, 2012
Revised: August 29, 2012
Published: August 29, 2012

dx.doi.org/10.1021/bi3005494 | *Biochemistry* 2012, 51, 7506−7514

trations of ITCs inhibit apoptosis while a high isothiocyanate dosage induces apoptosis.[24]

MIF, which has been found to have pro-tumorigenic, pro-angiogenic, and pro-inflammatory activities, is becoming widely recognized as a potential anticancer drug target. Small molecule inhibitors directed against MIF have been found to be useful both in animal models of sepsis[25] and in culture against cellular proliferation and migration of lung cancer cells[5] and restoration of contact inhibition in glioblastoma cells.[2] The reactivity of isothiocyanates against MIF therefore presents a natural nutritional targeting of an oncologically relevant protein, adding support to the rationale for the development of anti-MIF compounds for cancer chemotherapy. Herein, we quantitate the kinetics of the reactions of MIF with the nutrient isothiocyanates PEITC and sulforaphane. We also report the crystal structures and nuclear magnetic resonance (NMR) heteronuclear single-quantum coherence (HSQC) spectral changes of MIF complexed with these two ITCs and discuss their use for understanding the mechanism of MIF inhibition and further development of MIF inhibitors.

EXPERIMENTAL PROCEDURES

Materials. Recombinant human MIF and [^{15}N]MIF were expressed and purified as described previously.[25,26] L-Sulforaphane (the naturally occurring *R* configuration) and PEITC were purchased from Sigma-Aldrich (St. Louis, MO). [^{15}N]-Ammonium chloride was obtained from Cambridge Isotopes (Andover, MA).

MIF Derivatization Kinetics. Irreversible inhibition was observed by incubating MIF with inhibitor and diluting aliquots into assay buffer at various times to measure tautomerase activity as previously described for other covalently based inhibitors.[25] Kinetics of isothiocyanate derivatization of MIF were measured using 15 μM MIF incubated with or without 15 μM inhibitor in 2.9% DMSO, 19.4 mM Tris (pH 7.5), and 19.4 mM NaCl at room temperature (approximately 23 °C). Aliquots were assayed after incubation for 16 (±1), 90, 150, 240, 480, and 960 s. The MIF concentration during tautomerase assays was 0.20 μM, and the temperature of the spectrophotometer during the tautomerase assays was fairly stable (25−26 °C when assaying the tautomerase activity of the PEITC-derivatized MIF, 26−27 °C for sulforaphane-derivatized MIF, and 24−25 °C for the control incubation). Experiments were performed in triplicate for each inhibitor and for the control. Rate constants were calculated using GraphPad Prism 4.

Crystallization. PEITC and L-sulforaphane stock solutions were prepared in DMSO. A solution of 0.2 mM MIF, 1.0 mM isothiocyanate, 10% DMSO, 18 mM Tris (pH 7.5), and 18 mM NaCl was prepared and allowed to sit at ambient temperature on the bench for 2 and 5 min for PEITC and L-sulforaphane, respectively. The ITC/MIF solution was subjected to a few rounds of concentration and redilution in 20 mM Tris (pH 7.5) and 20 mM NaCl until the DMSO concentration was reduced to approximately 1% (for PEITC−MIF) or 0.5% (for sulforaphane−MIF). For crystallization, hanging drops were prepared by mixing 2 μL of 0.96 mM PEITC−MIF or 2 μL of 1.2 mM L-sulforaphane−MIF with 2 μL of reservoir consisting of 2 M $(NH_4)_2SO_4$, 0.1 M Tris (pH 7.5), and 3% 2-propanol. Pyramid-like crystals, 0.3−0.4 mm on a side, were grown at 20 °C.

Crystallographic Data Processing and Structure Determination. Diffraction data were collected on a Rigaku Micromax 007 X-ray generator with an R-Axis IV++ image plate detector. The data were processed using HKL2000.[27] The structure of each complex was determined by molecular replacement with AMoRe in CCP4[28,29] using protein coordinates from native MIF [Protein Data Bank (PDB) entry 3DJH] as a search model.[25] Initial models for the inhibitors were generated using the Dundee Prodrg Server. Refinement was performed using CNS,[30] and ligand placement and model building were performed using O and COOT.[31] Refinement statistics are listed in Table 1. Coordinates and crystallographic structure factors were deposited in the RCSB Protein Data Bank (entry 3SMB for PEITC−MIF and entry 3SMC for sulforaphane−MIF).

Table 1. Crystallographic Statistics

	PEITC−MIF	L-sulforaphane−MIF
	Integration and Scaling	
space group	$P2_12_12_1$	$P3_121$
unit cell	a = 67.49 Å, b = 67.67 Å, c = 87.77 Å, $\alpha = \beta = \gamma = 90°$	$a = b$ = 95.64 Å, c = 103.52 Å, $\alpha = \beta = 90°$, $\gamma = 120°$
resolution (Å) (highest shell)	90−1.6 (1.63−1.6)	110−1.8 (1.83−1.8)
no. of unique reflections	52662	51163
completeness (%)	97.9 (98.8)	99.9 (100)
redundancy	4.4 (4.3)	10.8 (10.4)
avg I/avg σ	20.31 (4.13)	25 (4.2)
R_{merge}	0.080 (0.277)	0.104 (0.502)
	Refinement ($F \geq 0$)	
no. of reflections	52638	51159
no. of atoms in the asymmetric unit	3074	3103
R_{work} (%)	18.1	17.2
R_{free} (%)	19.7	18.6
root-mean-square deviation from ideality[a]		
bond lengths (Å)	0.007	0.005
bond angles (deg)	1.3	1.3
average B factor (Å^2)		
overall	19.52	16.30
protein (no. of residues)	17.75 (114 × 3)	14.18 (114 × 3)
water	29.76 (434)	27.75 (446)
ions	36.52 (12)	30.67 (12)
inhibitor	17.53 (3)	23.43 (3)

[a]Compared to ideal bond lengths and angles as determined by Engh and Huber.[42]

NMR HSQC Experiments. ^{15}N-labeled MIF was covalently modified as described above and extensively dialyzed into 20 mM sodium phosphate buffer (pH 7.0) and 0.5 mM EDTA. Each NMR sample was prepared with 10% D_2O and protein concentrations of approximately 1 mM. All NMR experiments were conducted at 25 °C on a Varian INOVA 600 MHz spectrometer using a 5 mm triple-resonance probe equipped with triple-axis pulsed magnetic field gradients and utilized pulse sequences from the Varian BioPack User Library (Varian Inc., Palo Alto, CA). ^{1}H−^{15}N HSQC NMR spectra were processed using NMRPipe[32] with subsequent display and

dx.doi.org/10.1021/bi3005494 | *Biochemistry* 2012, 51, 7506−7514

analysis in Sparky[33] and with chemical shifts referenced indirectly to external 3-(trimethylsilyl)propionic-2,2,3,3-d_4 acid at 0.00 ppm.

RESULTS

Kinetics of MIF Derivatization by PEITC and L-Sulforaphane. MIF was incubated with an equimolar concentration of PEITC or L-sulforaphane, and the rate of enzyme inactivation was determined by measuring tautomerase activity after incubation for various times. MIF is a homotrimer with the three active sites formed by subunit interfaces. ITCs react with the catalytic proline in MIF with a stoichiometry of one ITC to one MIF monomer (Figure 1A,B). Therefore, the concentration of MIF used in the experiments was calculated as the total concentration of MIF monomeric subunits. Enzyme activity was fit to a hyperbolic curve (Figure 1C) to determine second-order rate constants according to eq 1,

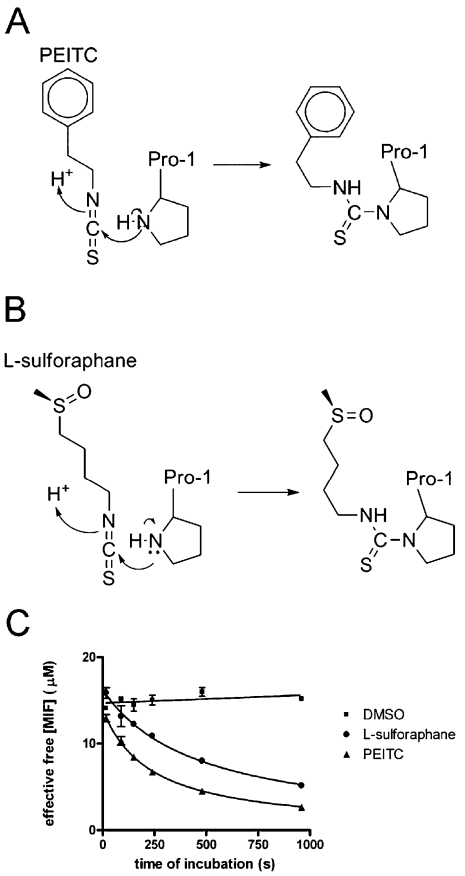

Figure 1. Kinetics of MIF reactivity with PEITC and L-sulforaphane. (A and B) Structures of PEITC (A) and L-sulforaphane (B) and the reactions they undergo with MIF, according to the known product of the reaction of isothiocyanates with proteins.[34] (C) MIF (15 μM) was incubated with an equal concentration of either PEITC or L-sulforaphane, or with vehicle (DMSO). At indicated times, the amount of remaining unreacted MIF, "effective free MIF", was assessed by measuring its tautomerase activity as described in Experimental Procedures. Data are plotted as means ± the standard error of the mean. In some cases, the error bars are smaller than the data symbols. The data were fit to a hyperbolic curve as described in the text. The calculated second-order rate constants for MIF derivatization are 3.1×10^2 M^{-1} s^{-1} with PEITC and 1.3×10^2 M^{-1} s^{-1} with L-sulforaphane.

$$y = \frac{A}{Akt + 1} \quad (1)$$

where A is the initial effective free MIF concentration (micromolar), t is the time (seconds) of MIF incubation with the inhibitor prior to enzymatic activity being assayed, and k is the second-order rate constant. PEITC covalently inhibits MIF with a rate constant of $(3.1 \pm 0.1) \times 10^2$ M^{-1} s^{-1}. The rate constant with sulforaphane is $(1.3 \pm 0.06) \times 10^2$ M^{-1} s^{-1}. As these compounds have the same reactive isothiocyanate group, the difference is due to the different R groups attached to the functional isothiocyanate moiety (Figure 1A,B).

Structure of the PEITC−MIF Complex. The 1.6 Å structure of the PEITC−MIF complex reveals that the phenylethyl group of the inhibitor occupies the hydrophobic active site of the protein (Figure 2A,B). The form of the inhibitor−enzyme adduct was modeled as the thiocarbamoylated protein (with the nitrogen of PEITC protonated and the double bond maintained between the carbon and sulfur atoms) based on known chemistry of isothiocyanates with amines. This chemistry has often been employed in the Edman degradation[34] and occurs not only with primary but also with secondary amines[35] and therefore is applicable to the N-terminal proline of MIF.

The torsion angle between the inhibitor and Pro-1 is 9.7 ± 2.5° [mean ± the standard deviation among the three active sites of the trimer (Figure 2B)]. Therefore, this represents a *cis*-thiopeptide bond. Such a complex would be less likely with any other N-terminal residue because of the stronger propensity for proline to form a *cis* peptide bond. Any energetic disadvantage of *cis* bond formation is evidently compensated by the affinity of the R group of PEITC for the MIF active site, as the hydrophobic chain is buried in the cavity.

Structure of L-Sulforaphane-Bound MIF. The structure of L-sulforaphane bound to MIF was determined at 1.8 Å resolution. In contrast to PEITC, which fills the active site cleft, the side chain of sulforaphane extends out of the binding site and resides at the surface of the protein (Figure 2C). This would suggest a lower affinity for the active site cleft of the aliphatic side chain of sulforaphane relative to that of the aromatic side chain of PEITC and is consistent with the slower rate constant for sulforaphane than PEITC for reacting with MIF. The covalent modification still occurs, highlighting the inherent reactivity of MIF with the isothiocyanate group. With the sulforaphane extending toward the protein surface, the bond formed with Pro-1 is in the *trans* conformation [ω = 171.3 ± 2.08°, mean ± SD (Figure 2C)]. One of the active sites lacks crystal contacts. At this site, although we see most of the sulforaphane, there is no electron density for the methylsulfinyl group of the inhibitor, indicating its mobility at the surface of the protein (Figure 2D). In the other two active sites, electron density is present for the entire inhibitor, presumably because of symmetry-related copies of the protein restricting the motion of the sulforaphane.

Structural Changes of MIF upon Binding Isothiocyanates. Comparison of the X-ray structure of sulforaphane-bound MIF to unbound MIF reveals there are no large structural changes in the active site (Figure 3A,B) or the trimer (Figure 4A). Although the chemical reaction pathway for the substrate undergoing the transition to product cannot be determined in this study, the product of this chemical reaction suggests the sulforaphane isothiocyanate group is in an ideal position for covalent bond formation with the amine of Pro-1

dx.doi.org/10.1021/bi3005494 | Biochemistry 2012, 51, 7506−7514

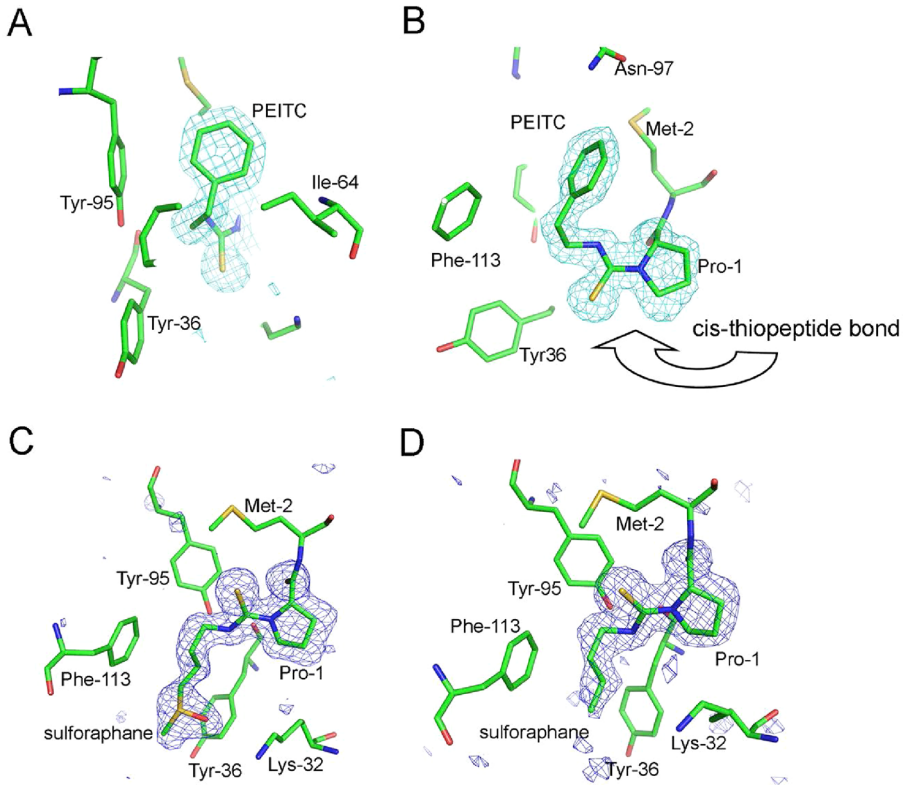

Figure 2. Structures of PEITC and sulforaphane bound to MIF. In all panels, both the inhibitor and Pro-1 were omitted from the electron density map calculations to remove crystallographic bias. (A and B) PEITC bound to Pro-1 in the active site of MIF. The 1.6 Å $F_o - F_c$ simulated annealing omit map is contoured at 4σ. Views were chosen to highlight the electron density of the PEITC aromatic ring (A) and the bond with Pro-1 (B). The active site shown is representative of all three active sites. (C and D) $F_o - F_c$ simulated annealing omit map (1.8 Å) of L-sulforaphane bound to MIF, contoured at 3σ. The electron density in panel C is representative of two of the active sites, in which crystal contacts place the inhibitor close to other MIF molecules in the crystal. The active site shown in panel D does not have nearby symmetry-related MIF molecules. The incomplete electron density for the inhibitor in panel D reveals the flexibility of sulforaphane when it is bound to MIF in the absence of crystal contacts. The views in panels B–D show the conformation of the inhibitor-protein bonds: *cis* when Pro-1 is bound to PEITC (B) and *trans* when Pro-1 is bound to sulforaphane (C and D).

because there is no significant movement of Pro-1 from its position in the apo structure. The structure of the MIF–PEITC complex, however, reveals a movement of Pro-1 within the active site (Figure 3B), but still no significant change in the trimer (Figure 4B). The position of the aromatic ring within the active site requires a conformational change in Pro-1 to make a covalent bond with PEITC. The disadvantage of the movement of Pro-1 and the *cis* conformation of the thiopeptide is overcome by the affinity of PEITC for the active site. The proline conformational change may explain why the kinetics of bond formation for PEITC, which makes more contacts with MIF in the active site and appears to have a greater affinity than sulforaphane, is not greater than 2.4-fold relative to that of sulforaphane.

It is also informative to compare sulforaphane and PEITC to two other irreversible inhibitors, 4-iodophenylpyrimidine [4-IPP (Figure 3C)] and phenylmethanesulfonyl fluoride [PMSF (Figure 3D)].[5,25] A similar Pro-1 shift attributed to PEITC is seen when MIF binds to 4-IPP but is not seen when MIF binds to PMSF. The difference in Pro-1 movement in PEITC and 4-IPP complexes relative to that of PMSF is due to their larger size and favorable contacts in the active site. Comparison of sulforaphane and PMSF complexed to MIF reveals the ψ angle for Pro-1 in PMSF changes to accommodate the tetrahedral covalent bond that is formed. Neither inhibitor yields any significant conformational change elsewhere in the protein (Figure 4).

NMR Studies of [^{15}N]MIF with PEITC and Sulforaphane. A previous NMR study of the reaction of MIF and another isothiocyanate, benzyl isothiocyanate (BITC), revealed large changes in ^{1}H–^{15}N peak width in the subunit interface indicative of a major conformational change.[8] We collected analogous ^{1}H–^{15}N HSQC NMR peaks using the same buffer and temperature on the covalently modified forms of MIF presented here and compared them to those of the unliganded protein. As can be seen in Figure 5A, both of the covalent modifications significantly perturb the backbone amide chemical shifts for ~50% of the residues. However, unlike what was reported for BITC, there were no detectable changes in line widths. Interestingly, the chemical shift changes induced by each of the covalent modifications were dissimilar in magnitude and direction. For the resonances that were not significantly perturbed by one covalent modification, they were also not affected by the other. In general, the pattern of backbone amide chemical shifts for the modified proteins remains consistent with a folded structural state. The distribution of backbone amide ^{1}H chemical shifts, with many values of >8 ppm, remains consistent with a high β-sheet content. One possible explanation for all of these observations involves rearrangement of the structural interface between MIF monomers within the trimeric complex. We hypothesize that

dx.doi.org/10.1021/bi3005494 | *Biochemistry* 2012, 51, 7506–7514

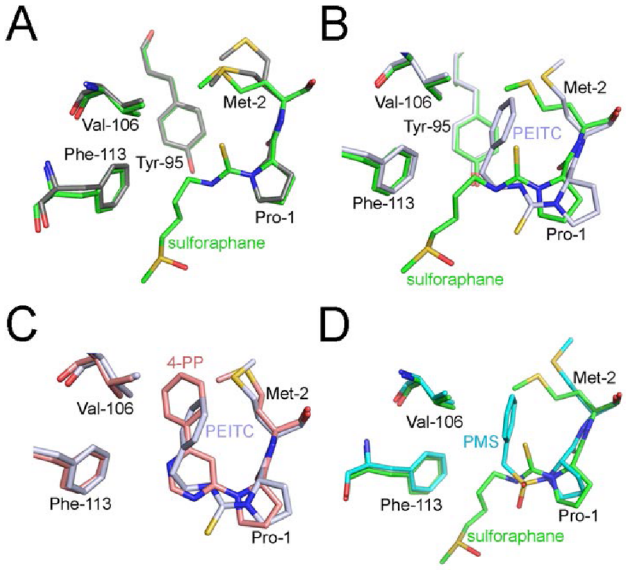

Figure 3. Effects of ITCs on MIF active site residues. All overlays were performed using a least-squares superposition of α-carbon atoms corresponding to residues 3−27, 37−50, 52−65, and 67−114. (A) Sulforaphane-derivatized MIF overlaid upon unliganded MIF (PDB entry 3DJH) reveals that there are no major conformational changes in the protein backbone. There are two conformations for Met-2 in the unliganded MIF. The side chain conformational difference seen in Tyr-36 is due to crystal contacts made by Tyr-36 in the active site of the sulforaphane−MIF complex. These Tyr-36 crystal contacts are not present in the unliganded MIF crystal form shown in the figure, which crystallized in a different space group. (B) Superposition of the sulforaphane−MIF complex onto the PEITC−MIF complex shows that PEITC displaces Pro-1 from its native position. (C) The Pro-1 displacement observed in the PEITC−MIF complex is similar to that observed upon reaction of MIF with 4-IPP [which leaves 4-phenylpyrimidine (4-PP) bound to the protein].[5] (D) ITC derivatization of MIF produces a planar proline imine (PDB entry 3B9S) nitrogen and therefore does not cause the bending in Pro-1 that is observed when MIF reacts with PMSF [which leaves a phenylmethylsulfonyl group (PMS) attached to the protein] that yields a tetrahedral imine (PDB entry 3CE4).

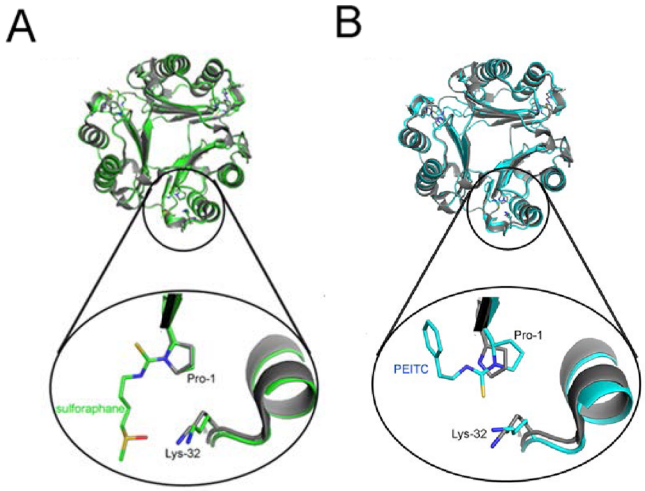

Figure 4. Binding to ITCs does not cause a conformational change in MIF. Superposition of sulforaphane−MIF (A) and PEITC−MIF (B) complexes onto unliganded MIF is shown. The top panels show the full trimeric protein, and the bottom panels show a close-up view of a representative active site, highlighting Lys-32. The position and orientation of Lys-32 do not undergo large changes upon ITC binding, and the global MIF tertiary structure remains unchanged. Overlays were performed as described in the legend of Figure 3.

the interface residues within the MIF trimer are able to exist in multiple conformations, without any associated perturbations of the overall secondary, tertiary, or quaternary structure. Covalent modification of the N-terminus, which is located within the interface, may alter the population distribution of structural states for these interface residues. In the case of BITC, the observed line broadening for interface residue backbone amides could be explained by conformational exchange on the NMR time scale induced by the covalent modification, which was not observed with sulforaphane or PEITC. Interestingly, noncovalent inhibitors at the active site also cause chemical shift broadening and changes in the positions of the chemical shifts.[7]

We used Sparky to overlay the peaks from both ITCs with those assigned from apo-MIF to produce a qualitative assessment of which residues moved upon formation of a covalent bond with the ITCs. More than 10% of the peaks from both ITCs superimposed very well with the apo-MIF peaks (e.g., see Val-41 at 8.77 and 127.61 ppm). We also included chemical shifts that were not perturbed significantly upon formation of the covalent bond with ITCs, those that partially overlapped or moved slightly relative to the apo-MIF peaks (Table S1 of the Supporting Information). We highlighted on the ribbon structure of apo-MIF all other residues corresponding to chemical shifts due to ITC covalent bond formation that were significantly perturbed or were absent relative to the apo-MIF peaks (Figure 5B). More than half the residues are perturbed and are mostly located around the active site at the subunit interface. These residues include the β-sheet and the hydrophobic residues from the α-helices that abut the β-sheet. A large portion of the C-terminal region, for example, interdigitates into the adjacent subunit and contributes one of the six strands in the β-sheet for each monomer. Perturbation of these C-terminal β-strands results in changes to the hydrophobic residues of the helix (helix II, residues 69−87) in the adjacent subunit. The lower half of other helix (helix I, residues 18−29) is perturbed because it is adjacent to β-strand I, directly following Pro-1. The loop (residues 30−37) that connects helix I to β-strand II possesses residues that are part of the active site and is also perturbed. The absence of chemical shift changes for more than half of the solvent-exposed helical residues distal to Pro-1 is an indication that the secondary and tertiary structure remains similar to those of the apo-MIF structure. The absence of chemical shift changes at this location also indicates that a large number of chemical shifts are due to subtle effects that are observed because of the sensitivity of NMR. However, this does not exclude changes in the conformation of MIF side chains due to covalent binding of the two ITCs.

DISCUSSION

The well-studied cancer-preventive effects of isothiocyanates are consistent with inhibition of the pro-inflammatory, pro-tumorigenic, and pro-angiogenic protein MIF. Covalent modification by ITCs obtained through the diet represents a natural mechanism for curtailing MIF-mediated cellular proliferation. Our observation that MIF is covalently modified by an ITC such as sulforaphane that extends out of the pocket is consistent with previous studies demonstrating that MIF is inhibited by a wide variety of ITCs, some containing aromatic

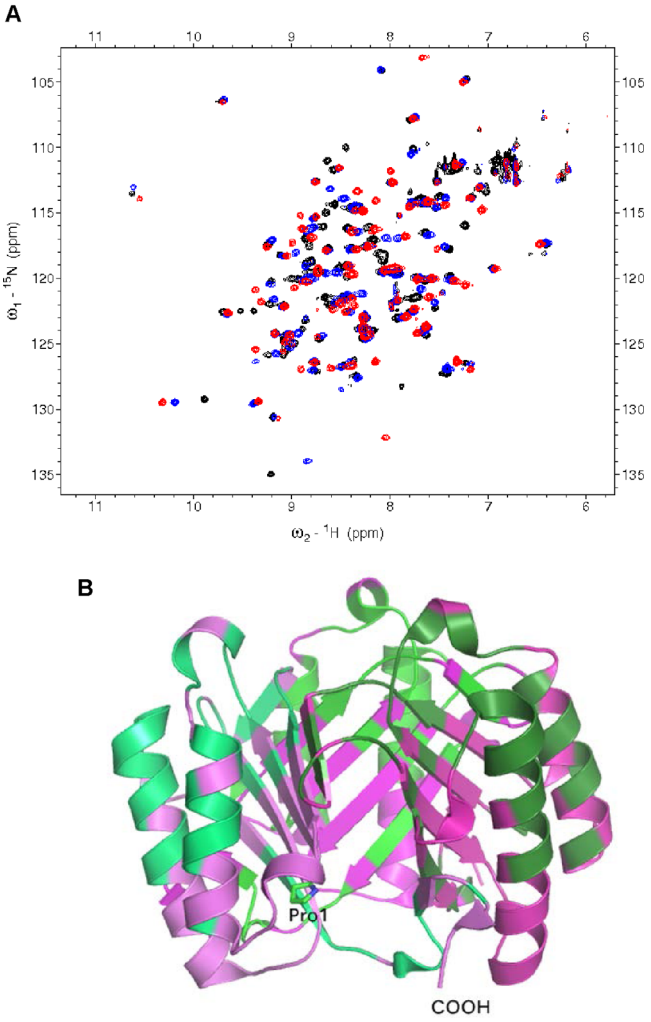

Figure 5. Analysis of NMR HSQC data. (A) Overlaid ^{1}H−^{15}N HSQC NMR spectra of [^{15}N]MIF (black contours) and L-sulforaphane-derivatized (blue contours) and PEITC-derivatized [^{15}N]MIF (red contours). All spectra were collected on a 600 MHz Varian Inova NMR spectrometer at 25 °C as described in Experimental Procedures. The dispersion of peaks in all three spectra is indicative of a high-β-sheet content protein, while the observed peak shifts upon derivatization are consistent with changes in the subunit interfaces of MIF. Unchanged NMR peak widths suggest a paucity of conformational and quaternary structural changes upon derivatization with PEITC and sulforaphane. (B) Ribbon diagram of the MIF trimer with backbone chemical shifts that are perturbed (magenta) or not perturbed (green), relative to the assigned apo-MIF chemical shifts, upon formation of a covalent bond with both sulforaphane and PEITC based on NMR HSQC experiments. Pro-1 and the C-terminus of the same subunit are labeled.

rings that are commonly seen binding in the MIF binding pocket and others that do not contain such moieties. This supports the theory that MIF inhibition plays a relevant role in the antitumorigenic effects of ITCs.[11,12] The more efficient in vitro derivatization of MIF by PEITC relative to sulforaphane contrasts with previously reported cellular activities. Cross et al. working with HeLa cells and Brown et al. working with Jurkat cells found sulforaphane inhibited tautomerase activity at lower concentrations than PEITC did when added to cells.[8,9] In these previously reported experiments, exogenous MIF was not added to the cells, and it is suggested that intracellular MIF was inhibited, as only lysates were assayed. The relative membrane permeabilities of sulforaphane and PEITC are not known and could explain the difference between the in vitro and cellular results, with sulforaphane penetrating the cellular membrane more efficiently than PEITC. There are other possible explanations that have yet to be studied. Among them are binding to other proteins with aromatic sites that sequester PEITC without any covalent modification and the half-life of PEITC and sulforaphane in cells.

ITCs demonstrate a kinetic profile similar to that of MIF inhibition by PMSF[25] except that the rates of covalent complex formation are much faster. (PMSF is so slow in modifying Pro-1 that a second-order rate constant would have been difficult to calculate, so pseudo-first-order kinetics.) PMSF binds within the active site, whereas sulforaphane extends outward. Therefore, the improved kinetics of sulforaphane versus that of PMSF must be due to the greater reactivity toward MIF of the ITC functional group relative to a fluorinated sulfonyl moiety. The MIF-binding R group of PEITC in the active site allows faster condensation with Pro-1 after the required proline movement is achieved relative to sulforaphane.

Condensation of an isothiocyanate with the N-terminus of a protein is the first step in the Edman degradation. However, Edman performed his original procedure at pH 8.6 to deprotonate the free amino terminus to allow the protein to react.[34] PEITC, however, reacts with MIF at near-neutral pH values. The complex was formed in pH 7.5 buffer in both the crystallization and kinetic experiments. The irreversible inhibition of MIF by PEITC is therefore dependent on the uniquely low pK_a of Pro-1,[36] which makes this protein a specific target of covalent ITC modification. Cross et al. found that MIF is the predominant protein modified by PEITC in HeLa cells by using a whole-cell proteomic labeling method.[9] Likewise, Brown et al. discovered that MIF is uniquely targeted by PEITC in Jurkat T-cells using a similar whole-cell lysate proteomic pull-down study.[8]

It is surprising that no large regional or global conformational changes were observed in the crystal structures upon binding of these two isothiocyanates. NMR HSQC experiments for probing changes upon MIF binding to BITC found changes in peak width due to exchange between multiple conformational species that are observed on the NMR time scale that mapped to a large region of the subunit−subunit interface indicative of a conformational change.[10] It also must be mentioned that other noncovalent inhibitors at the active site also had major HSQC changes but their X-ray structures were never determined.[7] The HSQC changes of PEITC and sulforaphane were examined under similar conditions. Although the NMR experiments with these two compounds did not lead to changes in peak width, most of the chemical shifts indicated a change in the subunit interface with no detectable changes in the secondary, tertiary, or quaternary structure of MIF (Figure 5). Given the sensitive nature of NMR experiments, these changes may not lead to a large rearrangement of the MIF structure but may indicate the existence of other, subtly different conformational states captured by each isothiocyanate in solution.

Although there are no major global changes of MIF modified by either ITC examined in this study, the structure of the PEITC-derivatized MIF indicates a local conformational change in Pro-1 (Figure 4). In silico modeling by Brown et al. suggested a change in backbone conformation in the vicinity of Pro-1 and Lys-32 in the presence of PEITC.[8] There is a movement of Pro-1 in the crystal structure but not nearly as

dx.doi.org/10.1021/bi3005494 | *Biochemistry* 2012, 51, 7506−7514

large as that predicted by modeling. There are no significant changes in Lys-32. Brown et al. found that PEITC reduced the affinity of a monoclonal antibody for MIF, which was interpreted as evidence of a protein conformational change even though the exact epitope was not known.[8] The same study, however, found a polyclonal serum to recognize PEITC-derivatized MIF and free MIF equally well. In light of our results, the epitope recognized by the monoclonal antibody could include the subunit interface or active site, which is modified by PEITC and thereby alters the epitope.

It was determined by Ouertatani-Sakouhi et al. that various ITCs interfere with binding of MIF to CD74.[10] This was attributed to the conformational change in MIF upon binding of BITC. Another possibility is that ITCs interfere with MIF−CD74 binding due to the covalent inhibitor physically blocking a portion of the CD74 binding site. This demonstrates the importance of the MIF tautomerase active site in its interaction with CD74, whether it is caused by direct binding to the active site or to other residues in the subunit interface that are affected by the binding of an inhibitor to the active site.

The efficiency with which isothiocyanate groups react with the active site of MIF provides a useful tool for deciphering structure−activity relationships (SAR). ITCs can be used to investigate how inhibitors with different functional groups affect MIF activity. Namely, inhibition of MIF biological activity conferred by ITCs that protrude from the active site can be compared to functional inhibition derived from those that bind in the active site. Such SAR data would provide information about how MIF interacts with receptors. One MIF-interacting compound has already been reported to enhance MIF biological activity.[37] Another example has to do with a parasitic (*Ancylostoma ceylanicum*) MIF (*Ace*MIF) that interacts with human CD74.[38,39] Characterization of inhibitors identified by targeting the *Ace*MIF active site revealed that the diuretic drug furosemide also inhibits *Ace*MIF−CD74 interactions. Removal of furosemide's sulfonamide and chloride groups protruding out of the active site and making no interactions with the protein allows the maintenance of a similar inhibition of tautomerase activity but fails to block *Ace*MIF−CD74 interactions. These examples involve compounds that interact with MIF noncovalently. An advantage of covalent inhibitors, such as ITCs, is that R groups can be modified while still maintaining irreversible binding to MIF. Once complete derivatization is achieved, any difference in receptor interaction of MIF modified by one ITC versus another is likely due to their respective effects on MIF−receptor interactions. The ITC scaffold therefore provides a convenient tool for attachment of various chemical moieties that extend into or out of the active site to different degrees and in different conformations. These potential reagents can be used to determine the range of enhancement or inhibition of binding and signaling of MIF receptors CD74, CXCR2, and CXCR4.[40] Therefore, this structural manipulation of the tautomerase active site, and presumably the subunit interface, can lead to insights regarding the nature of ligand−receptor interactions in MIF signaling.

Although we focus on the MIF interactions with cell surface receptors, there is substantial evidence that MIF is also an intracellular enzyme with an unknown substrate and product. It is ubiquitously expressed in every nucleated human cell and resides in the cytosol until the cell is stressed and exported in a signal sequence-independent pathway.[41] Proteins that have ∼30% identical sequences to human MIF are found in organisms such as *Arabidopsis thaliana*, *Caenorhabditis elegens*, and the marine cyanobacterium *Perkinsus marinus* and certainly do not express any of the known MIF receptors. Among the 30% identical residues are Pro-1 and some of the other human active site residues. All of this points to an enzymatic activity that may contribute to MIF's known biology. The modification of Pro-1 by isothiocyanates will certainly disrupt any enzymatic activity.

The NMR studies highlight the change in conformational states at the subunit interface upon inhibitor binding. The structural and kinetic aspects of this study underscore that MIF inhibition can be optimized for the design of more effective covalent inhibitors. The reactive ITC moiety can be coupled to MIF active site-binding groups that have increased affinity, thereby increasing potency and selectivity for covalent inhibitors. Structures of competitive inhibitors complexed to the active site may provide further insight into the design of more effective R groups.

■ ASSOCIATED CONTENT

Supporting Information

List of residues from either sulforaphane or PEITC that do have large changes in the NMR HSQC spectrum compared to that of apo-MIF (Table S1). This material is available free of charge via the Internet at http://pubs.acs.org.

■ AUTHOR INFORMATION

Corresponding Author

*Department of Pharmacology, Yale University School of Medicine, Box 208066, New Haven, CT 06520-8066. Phone: (203) 785-6233. Fax: (203) 785-5494. E-mail: elias.lolis@yale.edu.

Present Address

⊥Innovimmune Biotherapeutics, Inc., Brooklyn, NY 11226

Author Contributions

G.V.C. and C.F. contributed equally to this work.

Funding

This work was supported by National Institutes of Health Grants 5R01AI065029 and 5R01AI082295.

Notes

The authors declare no competing financial interest.

■ ACKNOWLEDGMENTS

We acknowledge Dr. Richard Bucala for helpful discussion.

■ ABBREVIATIONS

MIF, macrophage migration inhibitory factor; ITC, isothiocyanate; PEITC, phenethyl isothiocyanate; 4-IPP, 4-iodo-6-phenylpyrimidine; PMSF, phenylmethanesulfonyl fluoride; PMS, phenylmethylsulfonyl group; HPP, 3-(4-hydroxyphenyl)-pyruvate.

■ REFERENCES

(1) de Jong, Y. P., Abadia-Molina, A. C., Satoskar, A. R., Clarke, K., Rietdijk, S. T., Faubion, W. A., Mizoguchi, E., Metz, C. N., Alsahli, M., ten Hove, T., Keates, A. C., Lubetsky, J. B., Farrell, R. J., Michetti, P., van Deventer, S. J., Lolis, E., David, J. R., Bhan, A. K., Terhorst, C., and Sahli, M. A. (2001) Development of chronic colitis is dependent on the cytokine MIF. *Nat. Immunol. 2*, 1061−1066.

(2) Schrader, J., Deuster, O., Rinn, B., Schulz, M., Kautz, A., Dodel, R., Meyer, B., Al-Abed, Y., Balakrishnan, K., Reese, J., and Bacher, M. (2009) Restoration of contact inhibition in human glioblastoma cell lines after MIF knockdown. *BMC Cancer 9*, 464.

(3) Zhang, Y., Zeng, X., Chen, S., Zhang, Z., Li, P., Yi, W., Huang, H., Yao, J., Li, S., and Hu, C. (2011) Characterization, epitope identification and mechanisms of the anti-septic capacity of monoclonal antibodies against macrophage migration inhibitory factor. *Int. Immunopharmacol. 11*, 1333−1340.
(4) Crichlow, G. V., Cheng, K. F., Dabideen, D., Ochani, M., Aljabari, B., Pavlov, V. A., Miller, E. J., Lolis, E., and Al-Abed, Y. (2007) Alternative chemical modifications reverse the binding orientation of a pharmacophore scaffold in the active site of macrophage migration inhibitory factor. *J. Biol. Chem. 282*, 23089−23095.
(5) Winner, M., Meier, J., Zierow, S., Rendon, B. E., Crichlow, G. V., Riggs, R., Bucala, R., Leng, L., Smith, N., Lolis, E., Trent, J. O., and Mitchell, R. A. (2008) A Novel, Macrophage Migration Inhibitory Factor Suicide Substrate Inhibits Motility and Growth of Lung Cancer Cells. *Cancer Res. 68*, 7253−7257.
(6) Fingerle-Rowson, G., Kaleswarapu, D. R., Schlander, C., Kabgani, N., Brocks, T., Reinart, N., Busch, R., Schutz, A., Lue, H., Du, X., Liu, A., Xiong, H., Chen, Y., Nemajerova, A., Hallek, M., Bernhagen, J., Leng, L., and Bucala, R. (2009) A Tautomerase-null MIF Gene Knock-in Mouse Reveals that Protein Interactions and not Enzymatic Activity Mediate MIF-dependent Growth Regulation. *Mol. Cell. Biol. 29*, 1922−1932.
(7) Ouertatani-Sakouhi, H., El-Turk, F., Fauvet, B., Cho, M.-K., Pinar Karpinar, D., Le Roy, D., Dewor, M., Roger, T., Bernhagen, J., Calandra, T., Zweckstetter, M., and Lashuel, H. A. (2010) Identification and Characterization of Novel Classes of Macrophage Migration Inhibitory Factor (MIF) Inhibitors with Distinct Mechanisms of Action. *J. Biol. Chem. 285*, 26581−26598.
(8) Brown, K. K., Blaikie, F. H., Smith, R. A., Tyndall, J. D., Lue, H., Bernhagen, J., Winterbourn, C. C., and Hampton, M. B. (2009) Direct modification of the proinflammatory cytokine macrophage migration inhibitory factor by dietary isothiocyanates. *J. Biol. Chem. 284*, 32425−32433.
(9) Cross, J. V., Rady, J. M., Foss, F. W., Lyons, C. E., Macdonald, T. L., and Templeton, D. J. (2009) Nutrient isothiocyanates covalently modify and inhibit the inflammatory cytokine macrophage migration inhibitory factor (MIF). *Biochem. J. 423*, 315−321.
(10) Ouertatani-Sakouhi, H., El-Turk, F., Fauvet, B., Roger, T., Le Roy, D., Karpinar, D. P., Leng, L., Bucala, R., Zweckstetter, M., Calandra, T., and Lashuel, H. A. (2009) A new class of isothiocyanate-based irreversible inhibitors of macrophage migration inhibitory factor. *Biochemistry 48*, 9858−9870.
(11) Wattenberg, L. W. (1981) Inhibition of carcinogen-induced neoplasia by sodium cyanate, tert-butyl isocyanate, and benzyl isothiocyanate administered subsequent to carcinogen exposure. *Cancer Res. 41*, 2991−2994.
(12) Yang, M. D., Lai, K. C., Lai, T. Y., Hsu, S. C., Kuo, C. L., Yu, C. S., Lin, M. L., Yang, J. S., Kuo, H. M., Wu, S. H., and Chung, J. G. (2010) Phenethyl isothiocyanate inhibits migration and invasion of human gastric cancer AGS cells through suppressing MAPK and NF-κB signal pathways. *Anticancer Res. 30*, 2135−2143.
(13) Dey, M., Kuhn, P., Ribnicky, D., Premkumar, V., Reuhl, K., and Raskin, I. (2010) Dietary phenethylisothiocyanate attenuates bowel inflammation in mice. *BMC Chem. Biol. 10*, 4.
(14) Higdon, J. V., Delage, B., Williams, D. E., and Dashwood, R. H. (2007) Cruciferous vegetables and human cancer risk: Epidemiologic evidence and mechanistic basis. *Pharmacol. Res. 55*, 224−236.
(15) Tang, L., Zirpoli, G. R., Guru, K., Moysich, K. B., Zhang, Y., Ambrosone, C. B., and McCann, S. E. (2010) Intake of cruciferous vegetables modifies bladder cancer survival. *Cancer Epidemiol., Biomarkers Prev. 19*, 1806−1811.
(16) Tang, L., Zirpoli, G. R., Jayaprakash, V., Reid, M. E., McCann, S. E., Nwogu, C. E., Zhang, Y., Ambrosone, C. B., and Moysich, K. B. (2010) Cruciferous vegetable intake is inversely associated with lung cancer risk among smokers: A case-control study. *BMC Cancer 10*, 162.
(17) Jakubikova, J., Cervi, D., Ooi, M., Kim, K., Nahar, S., Klippel, S., Cholujova, D., Leiba, M., Daley, J. F., Delmore, J., Negri, J., Blotta, S., McMillin, D. W., Hideshima, T., Richardson, P. G., Sedlak, J., Anderson, K. C., and Mitsiades, C. S. (2011) Anti-tumor activity and signaling events triggered by the isothiocyanates, sulforaphane and phenethyl isothiocyanate, in multiple myeloma. *Haematologica 96*, 1170−1179.
(18) Musk, S. R., Astley, S. B., Edwards, S. M., Stephenson, P., Hubert, R. B., and Johnson, I. T. (1995) Cytotoxic and clastogenic effects of benzyl isothiocyanate towards cultured mammalian cells. *Food Chem. Toxicol. 33*, 31−37.
(19) Dinkova-Kostova, A. T., Fahey, J. W., Wade, K. L., Jenkins, S. N., Shapiro, T. A., Fuchs, E. J., Kerns, M. L., and Talalay, P. (2007) Induction of the phase 2 response in mouse and human skin by sulforaphane-containing broccoli sprout extracts. *Cancer Epidemiol., Biomarkers Prev. 16*, 847−851.
(20) Guo, Z., Smith, T. J., Wang, E., Sadrieh, N., Ma, Q., Thomas, P. E., and Yang, C. S. (1992) Effects of phenethyl isothiocyanate, a carcinogenesis inhibitor, on xenobiotic-metabolizing enzymes and nitrosamine metabolism in rats. *Carcinogenesis 13*, 2205−2210.
(21) Trachootham, D., Zhang, H., Zhang, W., Feng, L., Du, M., Zhou, Y., Chen, Z., Pelicano, H., Plunkett, W., Wierda, W. G., Keating, M. J., and Huang, P. (2008) Effective elimination of fludarabine-resistant CLL cells by PEITC through a redox-mediated mechanism. *Blood 112*, 1912−1922.
(22) Okazaki, K., Umemura, T., Imazawa, T., Nishikawa, A., Masegi, T., and Hirose, M. (2003) Enhancement of urinary bladder carcinogenesis by combined treatment with benzyl isothiocyanate and N-butyl-N-(4-hydroxybutyl)nitrosamine in rats after initiation. *Cancer Sci. 94*, 948−952.
(23) Okazaki, K., Yamagishi, M., Son, H. Y., Imazawa, T., Furukawa, F., Nakamura, H., Nishikawa, A., Masegi, T., and Hirose, M. (2002) Simultaneous treatment with benzyl isothiocyanate, a strong bladder promoter, inhibits rat urinary bladder carcinogenesis by N-butyl-N-(4-hydroxybutyl)nitrosamine. *Nutr. Cancer 42*, 211−216.
(24) Zanichelli, F., Capasso, S., Cipollaro, M., Pagnotta, E., Carteni, M., Casale, F., Iori, R., and Galderisi, U. (2012) Dose-dependent effects of R-sulforaphane isothiocyanate on the biology of human mesenchymal stem cells, at dietary amounts, it promotes cell proliferation and reduces senescence and apoptosis, while at anti-cancer drug doses, it has a cytotoxic effect. *Age (Dordrecht, Neth.) 34*, 281−293.
(25) Crichlow, G. V., Lubetsky, J. B., Leng, L., Bucala, R., and Lolis, E. J. (2009) Structural and kinetic analyses of macrophage migration inhibitory factor active site interactions. *Biochemistry 48*, 132−139.
(26) Cho, Y., Crichlow, G. V., Vermeire, J. J., Leng, L., Du, X., Hodsdon, M. E., Bucala, R., Cappello, M., Gross, M., Gaeta, F., Johnson, K., and Lolis, E. J. (2010) Allosteric inhibition of macrophage migration inhibitory factor revealed by ibudilast. *Proc. Natl. Acad. Sci. U.S.A. 107*, 11313−11318.
(27) Otwinowski, Z., and Minor, W. (1997) Processing of X-Ray Diffraction Data Collected in Oscillation Mode. *Methods Enzymol. 276*, 307−325.
(28) Collaborative Computational, Project Number 4 (1994) The CCP4 suite: Programs for protein crystallography. *Acta Crystallogr. D50*, 760−763.
(29) Navaza, J. (2001) Implementation of molecular replacement in AMoRe. *Acta Crystallogr. D57*, 1367−1372.
(30) Brunger, A. T., Adams, P. D., Clore, G. M., DeLano, W. L., Gros, P., Grosse-Kunstleve, R. W., Jiang, J. S., Kuszewski, J., Nilges, M., Pannu, N. S., Read, R. J., Rice, L. M., Simonson, T., and Warren, G. L. (1998) Crystallography & NMR system: A new software suite for macromolecular structure determination. *Acta Crystallogr. D54*, 905−921.
(31) Emsley, P., Lohkamp, B., Scott, W. G., and Cowtan, K. (2010) Features and development of Coot. *Acta Crystallogr. D66*, 486−501.
(32) Delaglio, F., Grzesiek, S., Vuister, G. W., Zhu, G., Pfeifer, J., and Bax, A. (1995) NMRPipe: A multidimensional spectral processing system based on UNIX pipes. *J. Biomol. NMR 6*, 277−293.
(33) Goddard, T. D., and Kneller, D. F. (2008) *Sparky 3*, University of California, San Francisco.

(34) Edman, P. (1949) A method for the determination of amino acid sequence in peptides. *Arch. Biochem. 22*, 475.
(35) Le, Z. G., Chen, Z. C., Hu, Y., and Zheng, Q. G. (2005) Organic reactions in ionic liquids: Ionic liquid-promoted efficient synthesis of disubstituted and trisubstituted thioureas derivatives. *Chin. Chem. Lett. 16*, 201−204.
(36) Swope, M., Sun, H. W., Blake, P. R., and Lolis, E. (1998) Direct link between cytokine activity and a catalytic site for macrophage migration inhibitory factor. *EMBO J. 17*, 3534−3541.
(37) Jorgensen, W. L., Gandavadi, S., Du, X., Hare, A. A., Trofimov, A., Leng, L., and Bucala, R. (2010) Receptor agonists of macrophage migration inhibitory factor. *Bioorg. Med. Chem. Lett. 20*, 7033−7036.
(38) Cho, Y., Jones, B. F., Vermeire, J. J., Leng, L., DiFedele, L., Harrison, L. M., Xiong, H., Kwong, Y. K., Chen, Y., Bucala, R., Lolis, E., and Cappello, M. (2007) Structural and functional characterization of a secreted hookworm Macrophage Migration Inhibitory Factor (MIF) that interacts with the human MIF receptor CD74. *J. Biol. Chem. 282*, 23447−23456.
(39) Cho, Y., Vermeire, J. J., Merkel, J. S., Leng, L., Du, X., Bucala, R., Cappello, M., and Lolis, E. (2011) Drug repositioning and pharmacophore identification in the discovery of hookworm MIF inhibitors. *Chem. Biol. 18*, 1089−1101.
(40) Bernhagen, J., Krohn, R., Lue, H., Gregory, J. L., Zernecke, A., Koenen, R. R., Dewor, M., Georgiev, I., Schober, A., Leng, L., Kooistra, T., Fingerle-Rowson, G., Ghezzi, P., Kleemann, R., McColl, S. R., Bucala, R., Hickey, M. J., and Weber, C. (2007) MIF is a noncognate ligand of CXC chemokine receptors in inflammatory and atherogenic cell recruitment. *Nat. Med. 13*, 587−596.
(41) Merk, M., Baugh, J., Zierow, S., Leng, L., Pal, U., Lee, S. J., Ebert, A. D., Mizue, Y., Trent, J. O., Mitchell, R., Nickel, W., Kavathas, P. B., Bernhagen, J., and Bucala, R. (2009) The Golgi-Associated Protein p115 Mediates the Secretion of Macrophage Migration Inhibitory Factor. *J. Immunol. 182*, 6896−6906.
(42) Engh, R. A., and Huber, R. (1991) Accurate bond and angle parameters for X-ray protein structure refinement. *Acta Crystallogr. A47*, 392−400.

■ NOTE ADDED AFTER ASAP PUBLICATION

This paper was published to the Web on September 11, 2012, with errors in the author affiliations. These were corrected in the version published on September 25, 2012.